

SMARTCATs STSM final report

A combined experimental and modeling study of the pyrolysis and oxidation of smart energy carriers: dimethoxymethane and decalin

1. Details of the STSM

Applicant details

Florence Vermeire

Florence.Vermeire@UGent.be

PhD student

Home Institute

Laboratory for Chemical Technology, Faculty of Engineering and Architecture, University of Ghent

Technologiepark 918, B-9052 Zwijnaarde, Belgium

Host Institute

Laboratoire Réactions et Génie de Procédés

1 rue Grandville – BP 20451, 54001 Nancy Cedex, France

2. Objective of the STSM

The aim of this Short Term Scientific Mission (STSM) is to extend the collaboration between the *Laboratorium voor Chemische Technologie (LCT)* and the *Laboratoire Réactions et Génie de Procédés (Nancy - France)* within the SMARTCATS COST Action (CM1404). The objectives of the proposed project are to perform experiments on the jet-stirred reactor, available in Nancy, to investigate the pyrolysis and combustion of oxygenated and cyclic model compounds. During the stay, experience with experimental apparatus, experience on kinetic model generation and the determination of kinetic and thermodynamic data will be exchanged.

3. Experiments performed during the STSM

During the STSM, experiments are performed on the isothermal quartz jet-stirred reactor. The investigated model compounds are dimethoxymethane and decalin. In this section, first a short description of the experimental apparatus is given, next the process conditions and results for both model compounds are summarized.

3.1. Experimental apparatus

Helium (99.99%), used as diluent, is mixed with the liquid fuel and passes through an evaporator. Afterwards, oxygen (99.999%) is added to the gaseous flow. The helium and oxygen flow rates are controlled by gas-mass-flow controllers (Bronkhorst) and the liquid fuel mass flow rate are regulated by liquid-Coriolis-flow controllers (Bronkhorst).

The gaseous mixture passes through an annular preheating zone, where it is heated to the reactor temperature, and enters the jet-stirred reactor through four nozzles. The nozzles and reactor are

designed to avoid thermal and concentration gradients. Thermocoax resistance wires provide heating for the annular preheating zone and the reactor. A type K thermocouple measures the temperature in the center of the reactor (measured temperature gradients < 5K). The pressure is set with a needle valve downstream of the reactor.

The reactor outlet is connected to 3 gas chromatographs that allow online quantification of product species. The transfer lines to the gas chromatographs are heated to avoid condensation. The first gas chromatograph is used to detect O₂, CO, CO₂ and CH₄ in case of oxidation and H₂ in case of pyrolysis. This gas chromatograph is equipped with a Carbosphere packed column and a thermal conductivity detector. The detector makes use of helium carrier gas in case of oxidation and argon carrier gas in case of pyrolysis, to allow the detection of H₂. The second gas chromatograph makes use of a PLOT-Q capillary column and a flame ionization detector preceded by a methanizer. The third gas chromatograph has a HP-5ms capillary column and a flame ionization reactor. The last gas chromatograph is available for either online or offline product identification. This gas chromatograph can be equipped with either a PLOT-Q or HP-5ms capillary column and has a quadrupole mass spectrometer. Product quantification for all GC's is done by injecting a known amount of the substance or with the use of the effective carbon number method. The relative experimental error on the compound mole fraction determined by injecting a known amount of the substance is 5% based on experience. In case the effective carbon number method is applied, the relative experimental error equals 10%.

3.2. *Dimethoxymethane*

Dimethoxymethane experiments are performed at both oxidation and pyrolysis conditions. For oxidation, three equivalence ratios are studied, $\phi=0.25, 1.0$ and 2.0 . The temperature for the experiments ranges from 500 K – 1100 K. Pressure is set to 1.07 bar, residence time to 2.84 s, for a reactor volume equal to 85 cm³, and DMM inlet mole fraction to 0.01. Little low temperature reactivity is obtained. For comparison, some experiments in the low temperature region (500K-800K) are performed at higher inlet mole fractions of DMM. No higher low temperature reactivity is observed. A total of 21 species are detected by the online GC's. The main products acquired from pyrolysis and oxidation experiments are identical, namely CO, CO₂, methane, ethylene, formaldehyde, and methylformate. A small peak during oxidation at fuel-lean conditions is present, indicating the presence of a cyclic ether most probably trioxane. Main product profiles are given in Figure 1. The carbon balances are close within 10% at all temperatures and equivalence ratios.

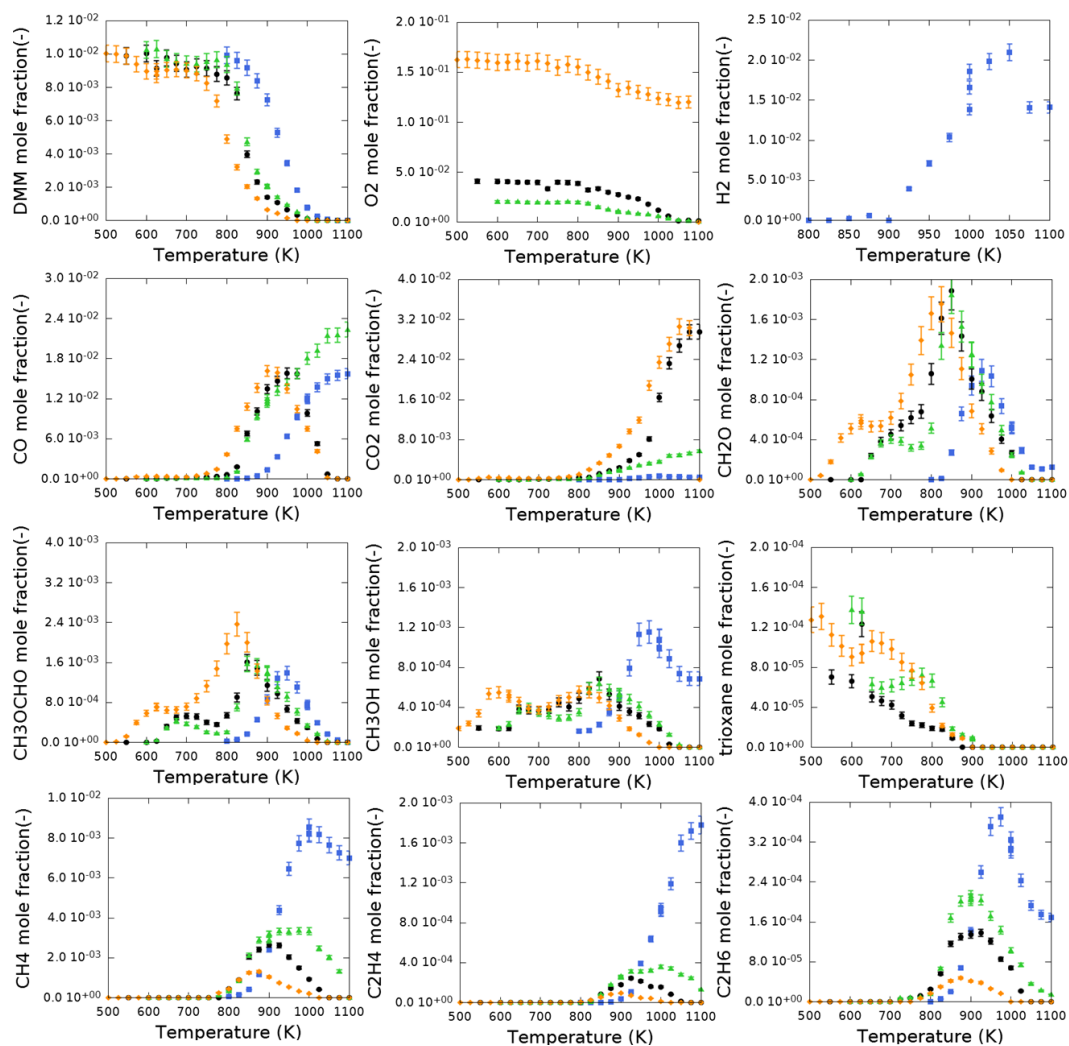


Figure 1. Experimental major product yields of DMM pyrolysis (blue■) and oxidation ($\phi=2.0$ green▲, $\phi=1.0$ black●, $\phi=0.25$ orange◆). Experimental conditions are $P=1.07$ bar, DMM inlet mole fraction 0.01 and residence time 2.84s for a reactor volume of 85 cm³. Experimental relative uncertainties are 5% for species calibrated with a known substance amount and 10% for calibration with the effective carbon number method.

3.3. Decalin

Experiments are performed to study the pyrolysis and oxidation of decalin in the JSR reactor. In case of oxidation, three equivalence ratios are studied, $\phi=0.5$, 1.0 and 2.0. The temperature for the experiments ranges from 500 K – 1100 K. Pressure is set to 1.07 bar, residence time to 2.0 s for a reactor volume equal to 85 cm³ and decalin inlet mole fraction to 0.004. During the pyrolysis experiments coke formation in the transfer lines to the gas chromatographs is detected. At low temperatures and low conversion, possible condensation of decalin occurred in the transfer lines. This complicates the decalin quantification at these temperatures. The most important peaks during pyrolysis and high temperature oxidation, a total of approximately 100 species, are integrated and identified. To improve identification, offline samples will be submitted to the GC×GC-TOF/MS. Preliminary results of the most important product species are given in Figure 2. To improve the carbon balances and the agreement between compounds measured by two GC's, the calibration of all compounds will be revised.

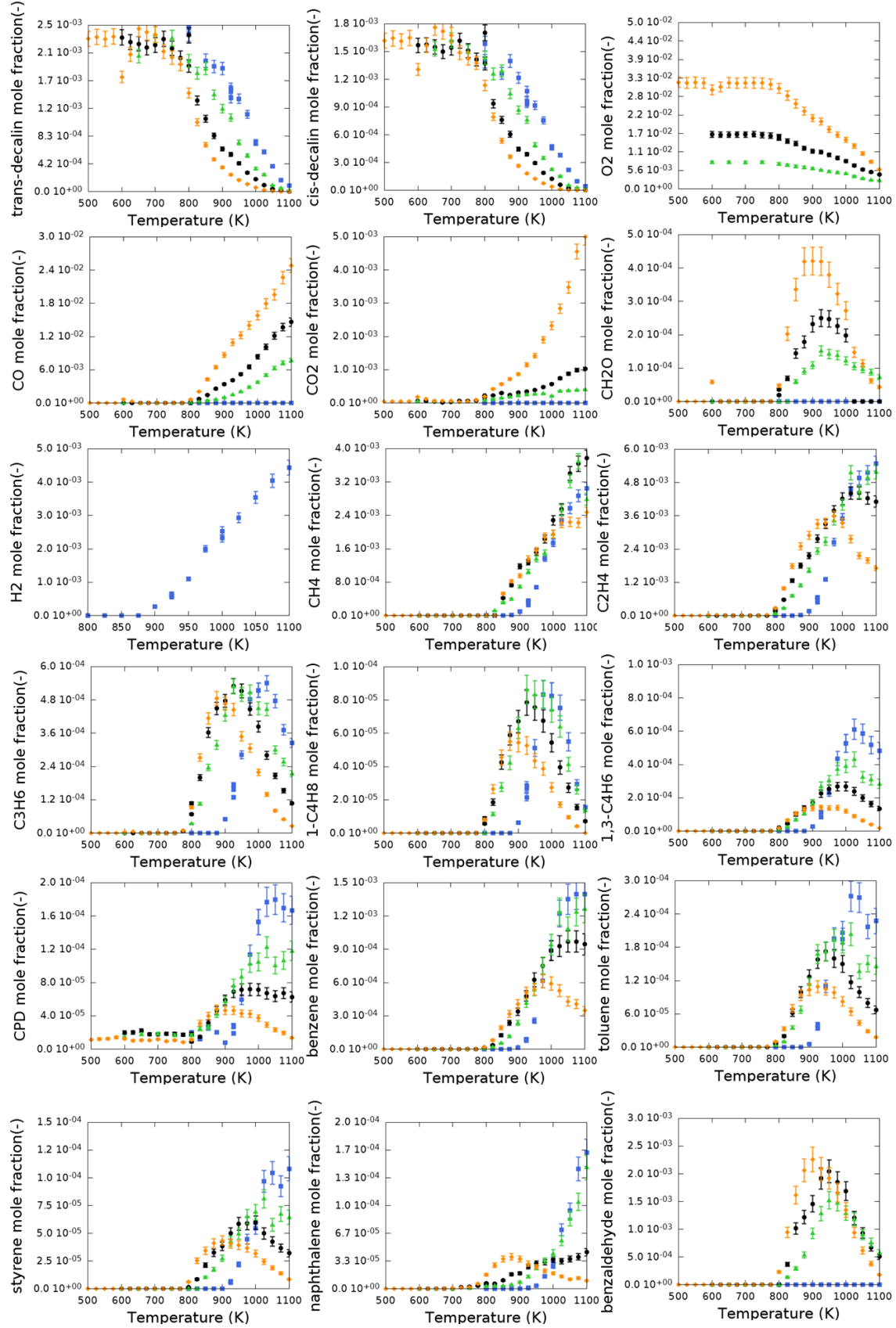


Figure 2. Experimental major product yields of decalin pyrolysis (blue■) and oxidation ($\phi=2.0$ green▲, $\phi=1.0$ black●, $\phi=0.5$ orange◆). Experimental conditions are $P=1.07$ bar, decalin inlet mole fraction 0.004 and residence time 2s for a reactor volume of 85 cm^3 . Experimental relative uncertainties are 5% for species calibrated with a known substance amount and 10% for calibration with the effective carbon number method.

Low temperature reactivity was obtained at the lowest equivalence ratios. A lot of peaks are observed at low temperature oxidation, indicating the presence of cyclic ethers and other low temperature oxidation products, such as aldehydes and ketones. Offline samples were taken at low temperature oxidation for possible identification of these oxygenates. The acquired chromatogram at $\phi=0.5$ and 600 K is shown in Figure 3.

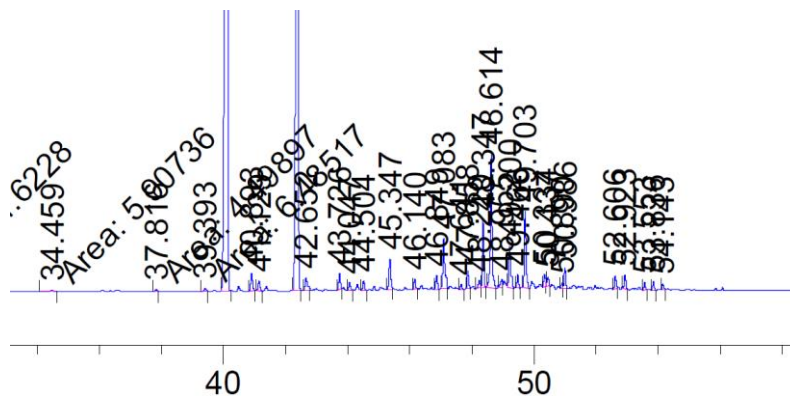


Figure 3. Part of the chromatogram acquired for oxidation of decalin at $\phi=0.5$ and 600 K.

4. Kinetic modeling during and after STSM

A kinetic model for the pyrolysis and oxidation of dimethoxymethane will be developed with the use of an automatic kinetic model generation tool called Genesys. Key reactions that are present during the pyrolysis and oxidation of dimethoxymethane are calculated with quantum mechanical techniques. In this section, the Arrhenius parameters resulting from the ab initio calculations are given and the model performance of the pyrolysis kinetic model is discussed. The kinetic model for oxidation is still under development.

4.1. First principles based Arrhenius parameters for dimethoxymethane pyrolysis and oxidation

Electronic structure calculations are performed with Gaussian 09, as implemented on the high-performance supercomputer at Ghent University, at the CBS-QB3 level of theory. The heat capacity at different temperatures, the standard entropy and the thermal contributions to the enthalpy are calculated from the Gaussian output file. All internal modes are treated as harmonic oscillators except for low frequency hindered rotors, which are approximated by 1-dimensional hindered internal rotations. All single bonds and bonds in the reactive moiety of the transition state are treated this way, except for the ones with a hindrance potential that exceeds 12 kcal/mol. These rotations are treated as harmonic oscillators. The hindrance potentials are calculated at the B3LYP/6-31G(d) level of theory with relaxed surface scans in which all coordinates, except for the considered dihedral angle, are re-optimized at each scan angle. The Fourier series expression of the hindrance potential together with reduced moment of inertia calculated at the $I^{(2,3)}$ level, as defined by East and Radom, are used to construct the Schrödinger equation for 1-dimensional internal rotation. The eigenvalues of the solution are used to determine the partition function as a function of temperature. The thermodynamic data is calculated from the total partition function after correction for the symmetry and the number of optical isomers. The conventional transition state theory is used to calculate the rate coefficients over a temperature range 300 K – 1500 K with 50 K increment. Tunneling is accounted for using the asymmetric Eckart potential. The resulting rate coefficients are regressed to a modified Arrhenius expression. The modified Arrhenius parameters for key reactions during dimethoxymethane pyrolysis and oxidation are given in Table 1. These

Arrhenius parameters will be used for the dimethoxymethane oxidation kinetic model. Ab initio calculations for sensitive reactions can be repeated at a higher level of theory, if required.

Table 1. First principles based Arrhenius parameters $k=AT^n\exp(-E_a/R/T)$ for key reactions during dimethoxymethane pyrolysis and oxidation.

Reaction	A [s^{-1} or $cm^3 mol^{-1} s^{-1}$]	n	E _a [$kcal mol^{-1}$]
	$5.04 \cdot 10^{+06}$	2.300	6.54
	$2.18 \cdot 10^{+10}$	1.155	6.54
	$2.55 \cdot 10^{+02}$	3.120	9.35
	$6.72 \cdot 10^{+05}$	2.097	9.61
	$2.03 \cdot 10^{-01}$	4.224	-5.70
	$1.00 \cdot 10^{+05}$	2.482	-3.67
	$1.32 \cdot 10^{+01}$	3.557	12.69
	$2.26 \cdot 10^{+02}$	3.163	11.77
	$3.34 \cdot 10^{+06}$	1.768	34.29
	$2.49 \cdot 10^{+14}$	-0.043	24.75
	$6.17 \cdot 10^{+08}$	1.29	13.66
	$5.37 \cdot 10^{+08}$	0.765	14.64
	$6.70 \cdot 10^{+07}$	0.585	14.12
	$1.85 \cdot 10^{+06}$	1.535	17.24
	$6.77 \cdot 10^{+11}$	0.320	13.02
	$3.39 \cdot 10^{+16}$	-1.230	23.37
	$5.02 \cdot 10^{+10}$	0.732	18.61
	$9.21 \cdot 10^{+13}$	-0.342	15.79
	$2.51 \cdot 10^{+16}$	-1.447	15.61
	$1.18 \cdot 10^{+13}$	-0.281	19.44

4.2. Pyrolysis kinetic model performance

The kinetic model for the pyrolysis of dimethoxymethane is developed with the use of the automatic kinetic model generation tool Genesys. Reaction families that are considered include fuel decomposition, hydrogen abstraction reactions, fuel isomerization reactions, β -scission

reactions and the reverse addition reactions. Arrhenius parameters for the fuel decomposition are used in analogy with similar reactions for dimethyl ether [1] and diethyl ether [2]. Arrhenius parameters for hydrogen abstraction reactions and β -scission reactions are either calculated with high level ab initio calculations or estimated with the group additive framework [3-8] implemented in Genesys [9]. The Genesys output is merged with a base mechanism to incorporate small species chemistry. Two base mechanisms are tested, *i.e.* aramomech 1.3 [10] and the propene oxidation mechanism developed by Burke et al. [11]. The model performance for both mechanisms is presented in Figure 4 for the most important species mole fractions. Reactor simulations are done using the perfectly stirred reactor model in CHEMKIN.

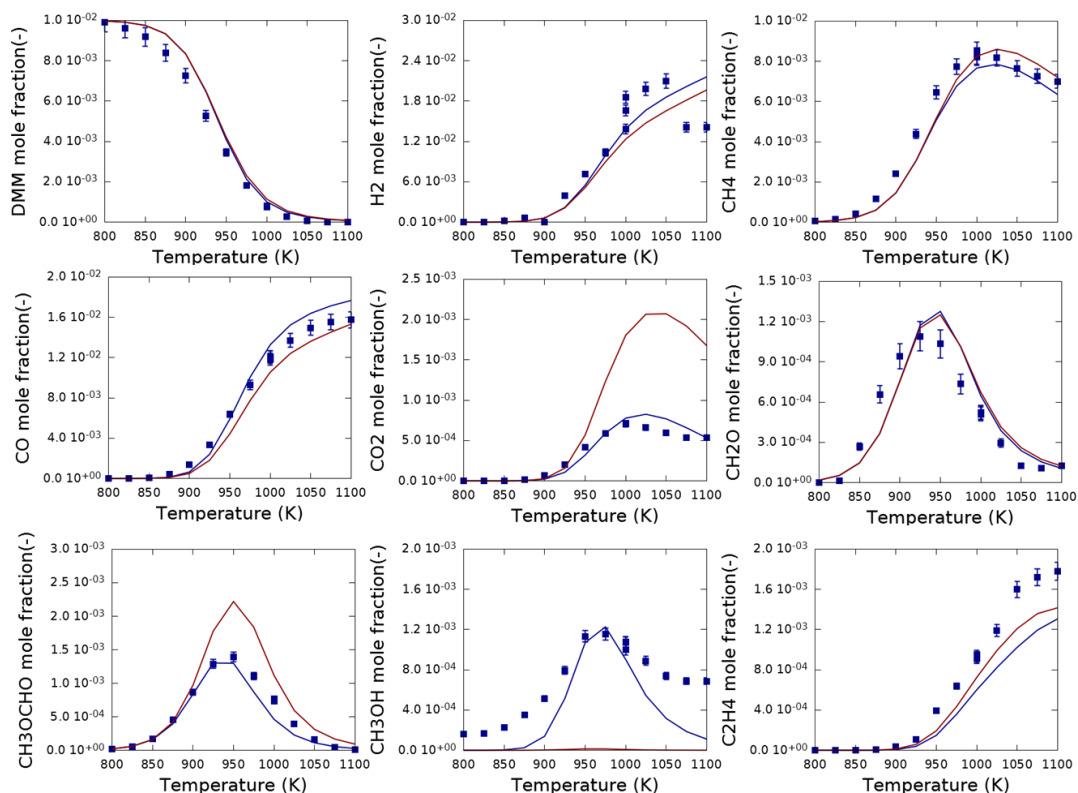


Figure 4. Model performance for dimethoxymethane pyrolysis experiments (blue squares). The kinetic model uses two different base mechanisms, *i.e.* aramomech 1.3 (blue lines) [10] and propene oxidation mechanisms by Burke et al. (red lines) [11]

Discrepancies between the two models are most pronounced for the CO, CO₂, methylformate (MF) and methanol mole fractions. These differences can be attributed to the different Arrhenius parameters for three key reactions during the pyrolysis of dimethoxymethane. In the propene oxidation mechanism by Burke et al. the first reaction indicated in Figure 5 is not present, the second and the third reaction are present, but the rate coefficients at 1000 K are very different from (i) the ones present in the other base mechanism considered, (ii) the ones reported by Huynh et al. [12] and (iii) the ones that are in-house calculated at the CBS-QB3 level of theory. After substitution of the Arrhenius parameters present in aramomech 1.3 for the three reactions, depicted in Figure 5, in the propene oxidation mechanism by Burke et al., the model performance is similar for both kinetic models.

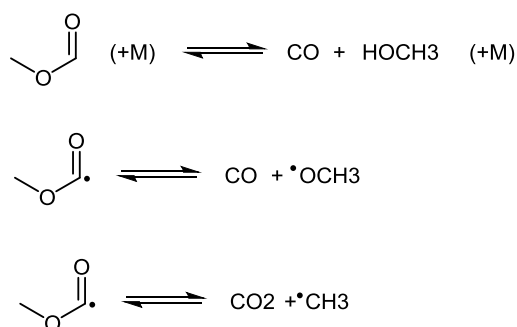


Figure 5. Key reactions during the pyrolysis of dimethoxymethane that have different Arrhenius parameters in the two used base mechanisms, *i.e.* aramcomech 1.3 [10] and propene oxidation mechanisms by Burke et al. [11]

5. Contribution to Action's aim

The core of the Action is the development of oxidation and pyrolysis kinetic models for fuels that have a potential to become new smart energy carriers. During the STSM, experiments for the pyrolysis and oxidation of 2 model compounds for smart energy carriers are performed. The first model compound is the most simple oxymethylene ether, *i.e.* dimethoxymethane. Oxymethylene ethers are produced from dimethyl ether, which can easily be formed from methanol dehydration. Because of their high cetane number and reduced soot and NO_x emissions, they are interesting fuel additives. The kinetic model that is developed for the pyrolysis and oxidation of dimethoxymethane contains new kinetic and thermodynamic data that can be used to extend databases for oxygen-containing species. The experimental data and kinetic model for second model compound, decalin, can contribute to the investigation of cyclic compounds that are present in for example pre-processed (deoxygenated) biomass. The increased formation of soot starting from these cyclic compounds and a kinetic model that is able to predict soot formation is a topic of interest.

6. Future collaboration

During future collaboration, a detailed kinetic model for decalin combustion will be developed. The kinetic model development will be in collaboration with the group of Frédérique Battin-Leclerc (host institute) and the group of William Pitz (Lawrence Livermore National Laboratory). Further details about the collaboration will be discussed over a Skype meeting.

The oxidation and pyrolysis of 3-carene will be investigated after purification of this compound. Pyrolysis experiments can be performed at the LCT in Ghent University. If possible, oxidation experiments will be performed in collaboration with KINCOM.

7. Confirmation by host institute of successful execution

The confirmation by the host institute is attached to the mail.

8. Resulting publications

An abstract and manuscript, concerning the pyrolysis and oxidation of dimethoxymethane, will be submitted for the 10th International Conference on Chemical Kinetics ICCK 2017. (<http://icck2017.engr.uic.edu/>)

The decalin pyrolysis and oxidation experiments will be published later in collaboration with Lawrence Livermore National Laboratory. Details concerning the collaboration still need to be discussed.

9. References

1. A. Rodriguez; O. Frottier; O. Herbinet; R. Fournet; R. Bounaceur; C. Fittschen; F. Battin-Leclerc, *Journal of Physical Chemistry A* 119 (28) (2015) 7905-7923 10.1021/acs.jpca.5b01939.
2. K. Yasunaga; F. Gillespie; J. M. Simmie; H. J. Curran; Y. Kuraguchi; H. Hoshikawa; M. Yamane; Y. Hidaka, *The Journal of Physical Chemistry A* 114 (34) (2010) 9098-9109 10.1021/jp104070a.
3. P. D. Paraskevas; M. K. Sabbe; M. F. Reyniers; G. B. Marin; N. G. Papayannakos, *Aiche J.* 62 (3) (2016) 802-814 10.1002/aic.15139.
4. P. D. Paraskevas; M. K. Sabbe; M. F. Reyniers; N. Papayannakos; G. B. Marin, *Chemphyschem* 15 (9) (2014) 1849-1866 10.1002/cphc.201400039.
5. P. D. Paraskevas; M. K. Sabbe; M. F. Reyniers; N. G. Papayannakos; G. B. Marin, *Journal of Physical Chemistry A* 119 (27) (2015) 6961-6980 10.1021/acs.jpca.5b01668.
6. M. K. Sabbe; M. F. Reyniers; V. Van Speybroeck; M. Waroquier; G. B. Marin, *Chemphyschem* 9 (1) (2008) 124-140 10.1002/cphc.200700469.
7. M. K. Sabbe; M. F. Reyniers; M. Waroquier; G. B. Marin, *Chemphyschem* 11 (1) (2010) 195-210 10.1002/cphc.200900509.
8. M. K. Sabbe; A. G. Vandeputte; M. F. Reyniers; M. Waroquier; G. B. Marin, *Physical Chemistry Chemical Physics* 12 (6) (2010) 1278-1298 10.1039/b919479g.
9. R. Van de Vijver; N. M. Vandewiele; P. L. Bhoorasingh; B. L. Slakman; F. Seyedzadeh Khanshan; H.-H. Carstensen; M.-F. Reyniers; G. B. Marin; R. H. West; K. M. Van Geem, *International Journal of Chemical Kinetics* 47 (4) (2015) 199-231 10.1002/kin.20902.
10. W. K. Metcalfe; S. M. Burke; S. S. Ahmed; H. J. Curran, *International Journal of Chemical Kinetics* 45 (10) (2013) 638-675 10.1002/kin.20802.
11. S. M. Burke; W. Metcalfe; O. Herbinet; F. Battin-Leclerc; F. M. Haas; J. Santner; F. L. Dryer; H. J. Curran, *Combustion and Flame* 161 (11) (2014) 2765-2784 10.1016/j.combustflame.2014.05.010.
12. L. K. Huynh; K. C. Lin; A. Violi, *Journal of Physical Chemistry A* 112 (51) (2008) 13470-13480 10.1021/jp804358r.